Simultaneous voltammetric determination of antihypertensive drugs nifedipine and atenolol utilizing MgO nanoplatelet modified screen-printed electrodes in pharmaceuticals and human fluids

CrossMark

Mohamed Khairy [a,*], Ahmed A. Khorshed [b,c], Farouk A. Rashwan [a], Gamal A. Salah [c], Hanaa M. Abdel-Wadood [c], Craig E. Banks [d,*]

[a] Chemistry Department, Faculty of Science, Sohag University, Sohag 82524, Egypt
[b] Department of Pharmaceutical Analytical Chemistry, Faculty of pharmacy, Sohag University, Sohag 82524, Egypt
[c] Department of Pharmaceutical Analytical Chemistry, Faculty of Pharmacy, Assiut University, Assiut 71526, Egypt
[d] Faculty of Science and Engineering, Manchester Metropolitan University, Chester Street, Manchester, M1 5GD, UK

ARTICLE INFO

ABSTRACT

Nifedipine and atenolol dugs are conjugated in several anti-hypertensive pharmaceutical formulations. Herein, a reproducible and sensitive voltammetric procedure has been developed for the simultaneous analysis of nifedipine and atenolol for the first time using MgO – nanoplatelets modified screen-printed electrodes (MgO – SPEs) via differential pulse voltammetry (DPV). Two very well-resolved and reproducible signals/oxidation peaks with a voltammetric separation of 0.35 V were obtained in Britton–Robinson (BR) buffer (pH 9). The MgO NPLs are found to exhibit a high electrocatalytic activity and improved voltammetric response compared to unmodified (bare) SPEs. Under optimum pH conditions (pH 9), the DPV curves exhibit linear responses to nifedipine and atenolol over the concentration ranges of 0.2–104.41 μM and 6.66–909.09 μM with detection limits of 0.032 μM and 1.76 μM, respectively. The applicability of the MgO-SPEs is successfully utilized for simultaneous determination of nifedipine and atenolol in pharmaceutical tablets and human urine samples with good accuracy and precision, these results agreeing with independent high-performance liquid chromatography (HPLC).

1. Introduction

Hypertension is the most prevalent cardiovascular disease in the world and affects as many as one quarter of the global adult population. Hypertension is an independent risk factor for stroke and coronary heart diseases [1]. The etiopathogenesis of hypertension is multifactorial; hence, several classes of anti-hypertensive drugs have been explored. To efficiently control high blood pressure levels, the use of antihypertensive combination drugs with complementary mechanism of actions has been markedly increased; therefore improving treatment compliance and adhesion have been performed rather than employing monotherapy [2] as recommended by the 2009 reappraisal of the European Society [3]. Calcium channel blockers and ß-blockers are complementary and their combination in lower concentration levels showed significantly blood pressure reduction compared to the maximum doses

of each ingredient [4]. Nifedipine (NIF) and atenolol (ATN) are a common combination to control high blood pressure [5,6]. NIF is a calcium channel blocker described as 3, 5- dimethyl 2,6-dimethyl-4-(2-nitrophenyl)-1,4-dihydropyridine-3,5-dicarboxylate and has commonly been used as a potent arterial vasodilator in the management of angina and cardiovascular diseases [7]. ATN is a beta-1 blocker chemically designed as (RS)-4-(2-hydroxy-3-isopropylaminopropoxy) phenylacetamide and is a primarily therapeutic drug for treatment of different cardiovascular disorders, such as cardiac arrhythmia and myocardial infarction [8]. These drugs combinations require highly restricted quality control in order to control alterations in their bioavailability and potency in *vivo*. Therefore, quantification of each active ingredient without the effect of interferences is highly recommended [9].

Various analytical techniques have been used for the determination of NIF and ATN separately such as spectrophotometry [10,11], spectrofluorimetry [12], chemilumeniscence [13] and voltammetry [14–21]. Lei Xu et al. have developed capillary electrophoretic methods with amperometric detection for the determination of ATN in urine samples [22]. The UV absorption spectra of NIF and ATN overlap precluding their simultaneous [23]. Therefore, the

analysts are turning to use the derivative and derivative ratio spectrophotometric methods for simultaneous determination of NIF and ATN. These methods show low signal, poor sensitivity, inconvenient signal-to-noise ratio, poor robustness and susceptibly to potential interferences form excipients. Many chromatographic methods have been reported for simultaneous quantification of NIF and ATN, however, high-cost, lack of portability, complex sample pre-treatment requirements, and inability to perform rapid in-field measurements limit their applicability [23–25]. For example, ATN was determined voltammetrically using bare/unmodified boron diamond doped electrodes (BDE) [14], carbon paste electrodes (CPE) modified with mordenite-type zeolite [17], amino acids assembly on gold nanoparticles (NPs) modified glassy carbon electrodes (GCE) [18], BiVO₄–Bi₂O₃/ITO electrodes [15] and CuO nanoparticle modified CPEs [19]. NIF was also determined by Ag NPs/GCE [20], Pd/Ag NPs alloy modified graphene nanoribbons [16] and β-cyclodextrin modified multi-walled carbon nanotube paste electrode [21]. Although these electrodes offered high selectivity for quantification of a single drug molecule, the continuous polishing, surface fouling, poisoning with time and decrease their sensitivity and reproducibility are still required; there is still an unmet need for a disposable, potentially portable electrochemical based sensing system which allows simultaneous determination of ATN and NIF drugs.

Nanomaterials have recently become one of the most exciting forefront field in analytical chemistry because they offer high effective surface-to-volume ratio, a unique ability to promote electron transfer, high catalytic efficiency and control over local microenvironment [26,27]. Therefore, nanomaterials acting as "electronic wires" to enhance the electron transfer between redox centres in the analyte and electrode surfaces [28]. Magnesium oxide (MgO) is a nontoxic, low-cost semiconductor [29], its optical band gap is about 5.40 eV [30]. MgO has large medicinal applications such as drug delivery, cell signalling and imaging and as a potent antimicrobial and antioxidant against resistant dreadful diseases [31,32]. Interestingly, magnesium ions change the bioavailability of NIF and ATN drugs and thus might interact with both anti-hypertensive drugs [33].

Herein, a simple and large-scale production of MgO NPLs has been developed *via* a gentle hydrothermal treatment of MgCl₂ within basic medium (pH 10). MgO NPLs have been dispersed and immobilised upon SPEs and utilized for the simultaneous determination of NIF and ATN in pharmaceutical tablets and urine samples. To the best of our knowledge, no study has been reported to date upon the simultaneous voltammetric determination of NIF and ATN in pharmaceutical formulations or biological fluids. Interestingly SPEs have inherent advantages such as miniaturization, versatility, low cost and the possibility of mass production [34]. Hence, simple modification of SPEs by MgO NPLs shows a simple, rapid, accurate, and validated analytical method for simultaneous quantification of NIF and ATN combination in pharmaceutical tablets Tenolat SR® and human fluids. The MgO-SPEs are independently validated using HPLC.

2. Experimental section

2.1. Reagents and materials

All chemicals were of the highest analytical grade available and were used as received without further purification from Sigma-Aldrich Company. All solutions were prepared using doubly distilled water of resistivity no less than 18.2 MΩ cm. NIF was kindly supplied by Sigma Pharmaceutical Co. (6th of October 2016, Egypt) and its purity value was (98.21 ± 1.22). ATN was kindly supplied by El Kahira Pharmaceutical Co. (6th of October, Egypt) and its purity value was (98.67 ± 1.54). Tenolat SR® (Sigma pharmaceutical Co., Cairo, Egypt) was labelled to contain 20.0 mg NIF and 50 mg ATN per tablet. The pharmaceutical formulations were purchased from local market. Solutions of Britton Robinson (B.R.) buffer of a wide pH range from 2 to 11 were prepared for the further studies.

2.2. Synthesis of MgO nanoplatelets (NPLs)

The synthesis of MgO NPLs was carried out by utilizing a typical hydrothermal procedure *via* hydrolysis of MgCl₂ (2.033 g dissolved in 50.0 mL water) in basic medium at pH 10. The solution was introduced into a 100.0 mL Teflon-lined, stainless steel autoclave. The autoclave was sealed and maintained at 160 °C for 12 h. The as-prepared white precipitate was collected and washed several times with water/ethanol mixture. The white precipitate was dried overnight at 45 °C and then calcined at 300 °C for 3 h.

2.3. Fabrication of screen-printed electrodes (SPEs)

The screen-printed graphite electrodes were fabricated at *Manchester Metropolitan University* utilizing appropriate stencil designs with a microDEK 1760RS screen-printing machine (DEK, Weymouth, UK) [35–38]. For each of the screen-printed sensors a carbon–graphite ink formulation (Product Code: product code: C2000802P2; Gwent Electronic Materials Ltd, UK) was first screen-printed onto a polyester flexible film (Autostat, 250 μm thickness). This layer was cured in a fan oven at 60° Celsius for 30 min. Next a silver/silver chloride (40:60) reference electrode was applied by screen-printing Ag/AgCl paste (Product Code: C2040308P2; Gwent Electronic Materials Ltd, UK) onto the plastic substrate. This layer was once more cured in a fan oven at 60° Celsius for 30 min. Last a dielectric paste ink (Product Code: D2070423P5; Gwent Electronic Materials Ltd, UK) was printed to cover the connections and define the 3 mm diameter graphite working electrode. After curing at 60° Celsius for 30 min the screen-printed electrode is ready to use. Similar screen-printed platforms have been electrochemically characterized in a previous contribution [35–38].

2.4. Preparation of MgO-SPEs and electrochemical measurements

Typically, 5 mg of MgO NPLs was mixed with 100 μL of 1% polytetrafluoroethylene (PTFE) and dispersed in 50 mL of deionized water for 30 min. 5 μL of this suspension was dropped onto the SPEs dried for one hour at 50 °C in the oven before the electrochemical experiments.

2.5. Characterization of MgO NPLs

The morphology of the MgO sample was investigated using field emission scanning electron microscopy (FE-SEM, JEOL model 6500). The MgO powder was ground and fixed onto a specimen stub using double-sided carbon tape. To obtain high-resolution micrographs, a 10 nm Pt film was coated on the magnesium oxide using anion sputtering (Hitachi E-1030) at room temperature. The SEM was operated at 15 KeV to obtain high-resolution SEM images.

Wide-angle powder X-ray diffraction (XRD) was performed by X-ray diffractometer (Model FW 1700 series, Philips, Netherlands) using with monochromatic Cu Kα radiation (λ = 1.54 Å), employing a scanning rate of 0.06°/min and 2θ ranges from 20° to 80°. The diffraction data were analysed using PDF software Released in 1996.

The voltammetric experiments were performed using Autolab 302N potentiostat/galvanostat workstation. All measurements were conducted using a three electrode configuration.

Cyclic voltammetry (CV) of MgO-SPEs was performed in potential range from −1.0 to 0.8 V at scan rate of 50 mV/s in B. R. buffer

solution of pH 9 until the electrochemical CV signal became stable. The optimum parameters for differential pulse voltammetry measurements are; deposition potential is − 0.5 V, deposition time is 5 s, modulation amplitude is 0.07 V, modulation time is 0.05 s, and step potential is 0.005 V.

Chromatographic measurement was carried out on an Autochro-3000 HPLC system (Younglin, Korea) equipped with UV detector, Rheodyne injection valve with a 20 μL loop. Monolithic column RP-18e 100 mm × 4.6 mm (Merck, Darmstadt, Germany) was employed for the separation. The mobile phase composed of (acetonitrile: 0.02 M phosphate buffer, pH = 4.0) (62.5: 37.5, v/v). The phosphate buffer was prepared by adding 10 mL of triethylamine to the prepared buffer (0.01 M). The pH adjusted using orthophosphoric acid. The mobile phase was prepared, filtered through 0.45 μm membrane filter and degassed for 10 min before use. The detection was carried out at wavelength 230 nm at flow rate 1.2 mL/min.

2.6. Applicability of MgO-SPEs for the determination of NIF and ATN in real samples

Ten tablets were accurately weighed and finely grinded in mortar. A chosen amount of this powder equivalent to 30 mg of NIF and 75 mg ATN was transferred into a 25 mL volumetric flask. About 20 mL of ethanol was added, swirled and sonicated for 5 min. The volume of the sample was completed to the mark and finally filtered using fine filter paper. The first portion of the filtrate was rejected. Specific volume of the drug stock solutions was diluted with ethanol to obtain a suitable concentration within linear calibration plot. Standard addition method has been utilized for determination of NIF and ATN in tablet.

The urine samples were taken from healthy peoples in Sohag University Hospital. All samples were diluted 30 times with BR solution of pH 9 before DPV measurements. The accuracy of the proposed DPV method was explored by spiking urine samples with different concentrations of NIF and ATN. The standard addition method was used for recovery determination of NIF and ATN in urine samples. The optimum conditions that was employed using RP C18 column and mobile phase composed of (acetonitrile: 0.02 M phosphate buffer, pH = 4.0) (62.5: 37.5, v/v). The detection was performed at wavelength 230 nm.

3. Results and discussion

3.1. Physical characterization of MgO NPLs

The morphology of the MgO samples, prepared as described in the experimental section, was investigated using scanning electron microscopy (SEM). SEM images show a highly dispersed and uniform hexagonal platelet-like morphology (Fig. 1a). The average size of hexagonal platelet is found to corresponding to an average width of ~200 nm with a thickness of 30 nm. Fig. 1b shows the XRD pattern of MgO sample. The diffraction peaks can be indexed to the cubic lattice of MgO (JCPDS No. 4-829), with the characteristic peaks at (111), (200), (220), (311), and (222). This result indicates that the MgO is in a pure crystalline material with no impurities.

3.2. Electrochemical characterization of MgO-SPEs

The electrochemical performance of the MgO NPLs modified screen-printed electrodes (MgO-SPEs) have been investigated and directly compared to unmodified (graphite) screen-printed electrodes (SPEs) using cyclic voltammetry and electrochemical impedance spectroscopy. Fig. 2 shows the cyclic voltammograms and complex plan plots of 0.3 mM of potassium ferroyanide $K_4[Fe(CN)_6]$ in 0.1 KCl using unmodified SPEs and MgO-SPEs. It is

Table 1
Simulation of impedance data *via* equivalent circuit model.

Parameters	SPEs	MgO-SPEs
R1/Ω	1000	1000
R2/kΩ	19	10
AW1/kΩs$^{-1/2}$	18	10
P1/μF	2.5	2.0
n1	0.8	0.8

R1 is solution resistance, R2 is charge transfer resistance, AW1 is Warburg impedance, P1 is capacitance and n1 takes value from 0 to 1.0 to describe the constant phase element.

found that the potential peak separation corresponds to 412 mV and 314 mV at a scan rate of 50 mV (*vs.* Ag/AgCl) for the unmodified SPEs and MgO-SPEs, respectively. In order to evaluate the effect of MgO NPLs upon the SPE's heterogeneous electron transfer properties, it is possible to employ the Nicholson's method [39]. It is widely used to estimate the heterogeneous rate constant ($k°$) for quasi-reversible electrochemical reactions *via* the following equation:

$$\Psi = k^o\{\pi Dn\upsilon F/RT\}^{-1/2}$$

where Ψ is a kinetic parameter, D is the diffusion coefficient for $[Fe(CN)_6]^{3-/4-}$ (7.60×10^{-6} cm^2 s^{-1}), n is the number of electrons transferred in the reaction, υ is the scan rate, F is the faraday constant, R is the gas constant, and T is the Temperature (Kelvin). Ψ is deduced from ΔE_P (the peak-to-peak separation) for a one electron process at a set temperature (298 K). For practical usage, the function of $\Psi(\Delta E_P)$ could fits Nicholson's data as given by: $\Psi = (-0.6288 + 0.0021X)/(1 - 0.017X)$, where X = ΔE_P is used to determine Ψ as a function of experimentally obtained ΔE_P values at various voltammetric scan rates [40]. It is therefore possible to produce a graph, whereby Ψ is plotted against $[\pi Dn\upsilon F/RT]^{-1/2}$, and the standard heterogeneous rate constant ($k°$) can be determined via the gradient. In cases where the ΔE_P exceeds a value of 212 mV, the following equation should be considered:

$$k^° = \left[2.18\left(\alpha Dn\upsilon F/RT\right)^{1/2}\right] Exp\left[-\left(\frac{\alpha^2 nF}{RT}\right)x\Delta E_P\right]$$

where α is assumed to be 0.5. The heterogeneous rate constants were determined to be 8.21×10^{-4} and 1.72×10^{-3} cm s^{-1} for SPEs and MgO-SPEs, respectively [40]. MgO NPLs enhanced the electrochemical performance and facilitate the electron transfer rate of the graphite screen-printed electrode in order of 2 times.

The complex plan plots of unmodified SPEs and MgO-SPEs in $K_4[Fe(CN)_6]$/0.1 M KCl represented also the enhanced electrochemical performance in presence of MgO NPLs. The applied DC-voltage is about 0.35 V (*vs.* Ag/AgCl), the excitation voltage applied to the electrochemical cell was 5 mV and the frequency range was from 100 kHz to 0.1 Hz. The Nyquist plots showed a semicircle followed by straight line, which reveal direct electron transfer (Fig. 2b). The simulation of the impedance spectra involved ohmic solution resistance (R1), charge transfer resistance (R2), Warburg impedance (W1) for diffusion of $[Fe(CN)_6]^{4-}$ in KCl solution and P1 and n1 are related to constant phase element (CPE) of a double layer capacitance. As shown in Table 1, the charge transfer resistance and Warburg impedance were significantly decreased confirming an effective an MgO-mediated charge transfer process at SPE surfaces.

3.3. Electrochemical behaviours of NIF and ATN using MgO NPLs

Screen-printing was utilized to fabricate economic, sensitive, reproducible, portable and disposable electrochemical sensors, which is advantageous since this approach offers online field detection [35–38,40]. Different nanostructure materials such as BiO [41],
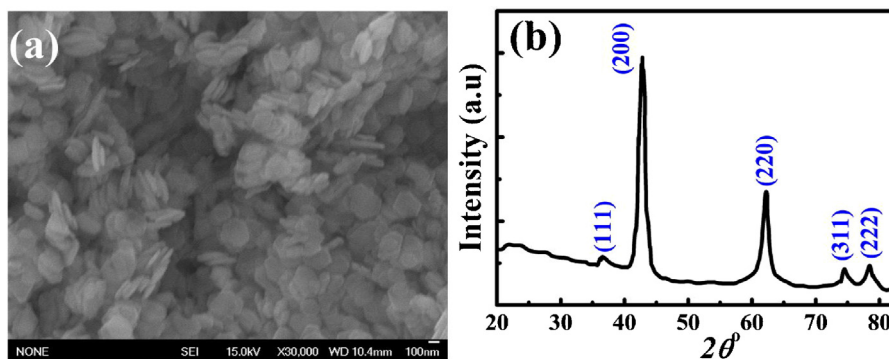
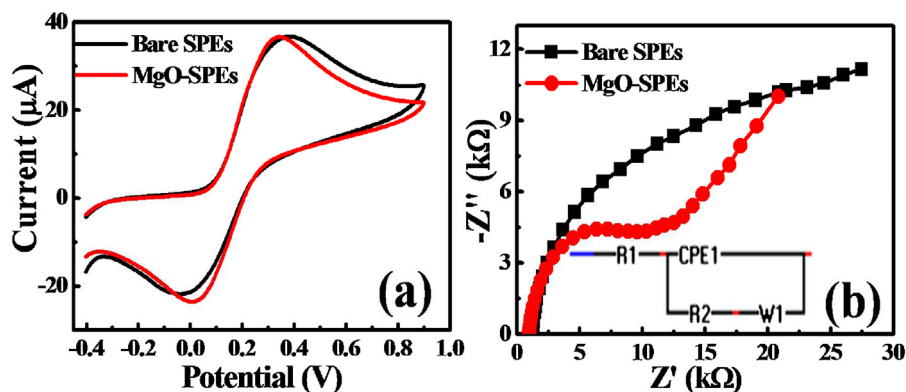**Fig. 1.** SEM image (a) and XRD pattern (b) of the fabricated MgO nanoplatelets.

Fig. 2. (a) Typical cyclic voltammetry curves and (b) complex plan plot of 0.3 mM $K_4[Fe(CN)_6]$ in 0.1 M KCl at unmodified SPEs and MgO − SPEs [Inset: The equivalent circuit describes the electron transfer process at the two SPE surfaces].
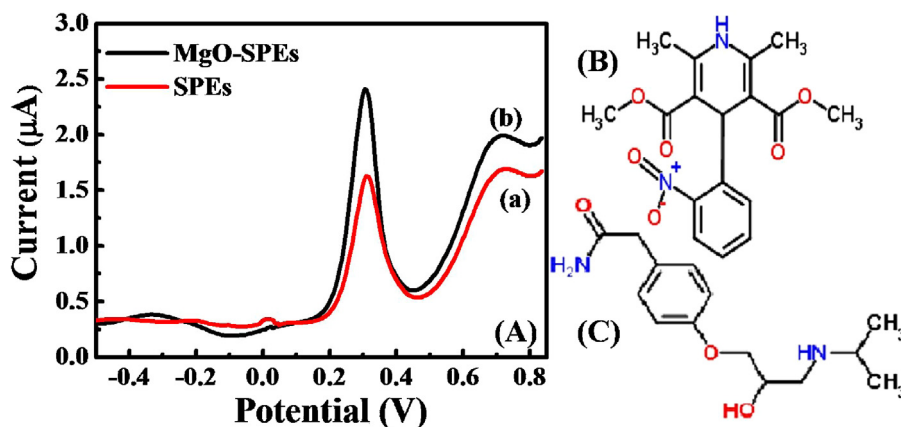

Fig. 3. (A) DPV curves of 25 μM NIF and 131 μM ATN both simultaneously present in pH 9 using (a) unmodified SPEs and (b) MgO − SPEs. (B) and (C) are the chemical structures of NIF and ATN, respectively.

NiO [42], CuO [36], ZnO [43], carbon nanotube (CNT) and MgO were investigated for determination of NIF and ATN. It was found that MgO shows a promising nanostructure material for simultaneous determination of NIF and ATN (Fig. S1 (a, b)). MgO NPLs were fabricated as described in the experimental section. Fig. 3 shows typical differential pulse voltammograms of 25 μM NIF and 131 μM ATN comparing the response of unmodified SPEs and MgO-SPEs in B.R. buffer pH 9. The MgO-SPEs shows great improvement of the electrochemical response of NIF and ATN (Fig. 3) compared to the unmodified/bare SPE indicating that the MgO nanoplatelets offer enhanced electron transfer characteristics.

The choice of a suitable medium/electrolyte is very important in electroanalytical research since it is greatly influenced the ana-

lytical response of analytes. The electrochemical behaviours of NIF and ATN have been studied using MgO-SPEs over a wide range of pH values, namely, 2–11. Fig. S2 shows the electrochemical behaviours of 66 μM NIF and 322 μM ATN on MgO-SPEs recorded in different pH values. Generally, the pH dependence of the voltammetric response shows an increase in the intensity of the anodic peak current in basic buffer solutions for both drugs. ATN did not show any electrochemical response below pH 6 due to the protonation of its amino group [44]. The B.R. buffer solutions of pH 7 and pH 9 were used to determine NIF and ATN, separately. Well-defined voltammetric anodic peaks were presented at 0.49 V and 0.70 V for NIF and ATN in pH 7 and pH 9, respectively. The difference in oxidation peak potentials of NIF and ATN was about 0.35 V in pH 9 com-
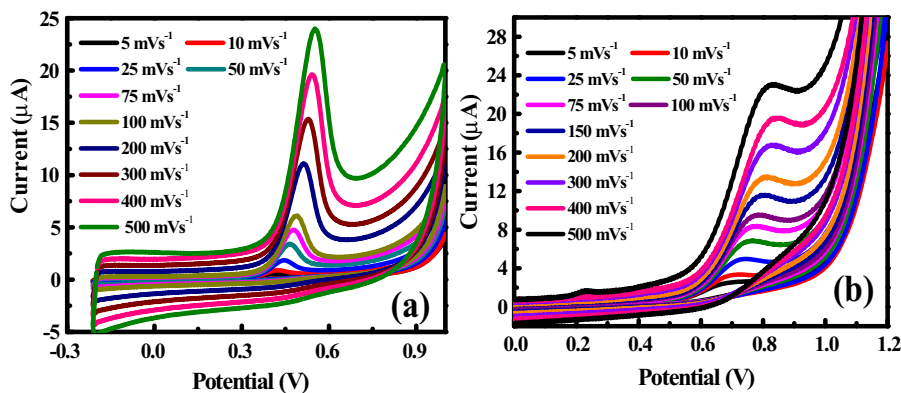
Fig. 4. CV curves of 66 μM NIF (a) and 322 μM ATN (b) in B.R. buffer solution using MgO −SPEs in pH 7 and pH 9, respectively.
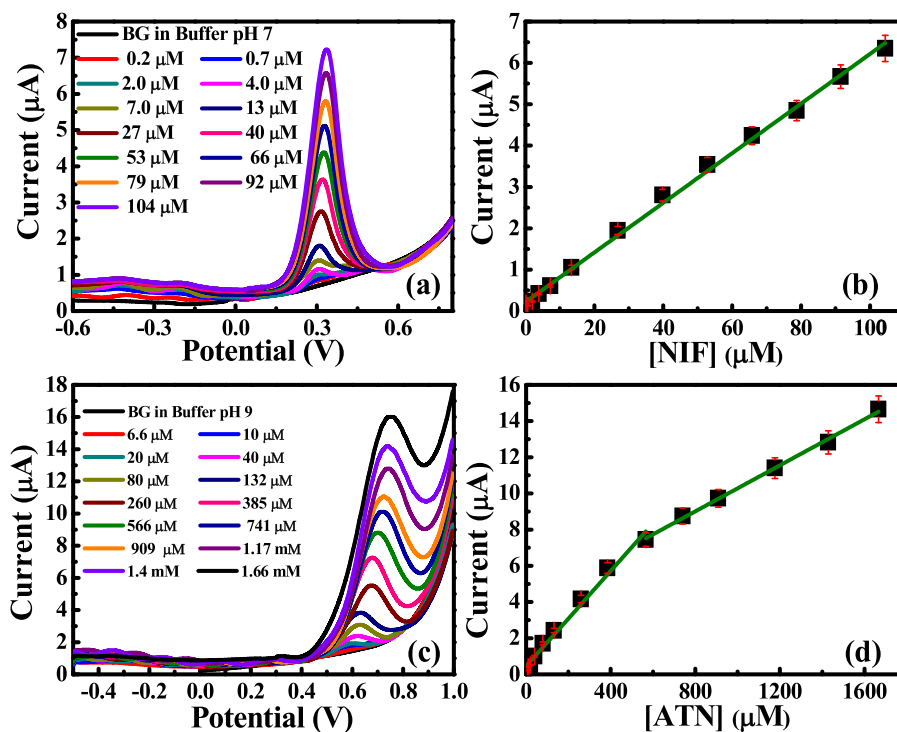

Fig. 5. DPV curves of NIF (a) and ATN (c) additions in B.R. buffer pH 7 and pH 9 respectively, linear correlation of oxidation peak current and concentrations of NIF (b) and ATN (d). [DPV parameters: Step potential = 0.005 mV, modulation amplitude = 0.07 V modulation time 0.05 s, interval time = 0.1s, scan rate = 0.05 mVs⁻¹].

pared to 0.25 V in pH 7. Therefore, pH 9 was selected as suitable pH value to determine both NIF and ATN in pharmaceutical dosage and human fluids. The oxidation peak potentials for NIF and ATN shifted toward less positive values with increasing the solution pH, indicating protons participation in the electrochemical processes. The slope of linear relationship between E_p and pH was found to be 51 mV/pH and 54 mV/pH for NIF and ATN, respectively. These values are very close to Nernstian slope (59 mV/pH at 298 K) for a process that involves the transfer an equal number of protons and electrons in the electrochemical mechanism.

Fig. 4 shows the cyclic voltammetric curves of 66 μM NIF (Fig. 4a) and 322 μM ATN (Fig. 4b) in B.R. buffer solution pH 7 and pH 9 respectively using MgO-SPEs over the range of scan rates 5 − 500 mV/s. The peak currents of NIF and ATN are found to increase with increasing voltammetric scan rates. As shown in Fig. S3, the oxidation peak current of NIF is linearly correlated with scan rates; $I_{NIF}/\mu A = 0.92\,(\upsilon/Vs^{-1}) - 38.51\,\mu A; R^2 = 0.99$. However, the oxidation peak current of ATN is linearly correlated with square root of scan rate; $I_{ATN}/\mu A = 0.36\,(\upsilon/Vs^{-1})^{0.5} + 22.55\,\mu A; R^2 = 0.99$. This behaviour

reveals that, the electrochemical oxidation of NIF is governed by adsorption process while ATN is under a diffusion controlled process. A small shift in the peak potential toward positive direction was also observed which confirms the irreversibility nature of the electrode processes.

3.4. Determination of NIF and ATN using MgO-SPEs

The instrumental parameters in the DPV experiments such as deposition potential, deposition time, modulation amplitude, modulation time, interval time and step potential have been optimized in BR buffer solution (pH 9.0) containing the mixture of 16 μM NIF and 160 μM of ATN. The optimum DVP parameters were found to be: deposition potential, −0.5 V; deposition time, 5s; modulation amplitude, 0.07 mV; modulation time, 0.05 s; interval time, 0.1s; scan rate, 0.05 mVs⁻¹; and step potential 0.005 V. Fig. 5 shows DPV curves for the consecutive additions of concentrations of NIF over the range of 0.20 μM − 104.41 μM and ATN concentrations over the range of 6.67–1660 μM into B.R. buffer solution of pH

Table 2
Comparison of various voltammetric methods for independent determination of ATN and NIF with the previous works.

comment	Refs.	Supporting electrolyte	Real sample	LOD (μM)	Linear range (μM)	Drug	Electrode
-Difficult to apply infield -Small linear concentration range -Electrode Poisoning and fouling with time	[19]	0.15 M B. R. Buffer	serum	1.12	12–96	ATN	**CuO NPs/CP**
-Tedious fabrication process -Difficult to apply infield -Expensive electrode materials	[15]	0.25 M NaNO$_3$	Tablet Urine	0.459	50 –800	ATN	**BiVO$_4$–Bi$_2$O$_3$/ITO**
-Small concentration range -Electrode Poisoning and fouling with time	[17]	Acetate buffer pH5	Tablet Urine	0.10	0.4 to 80	ATN	1 Mordenite/CP
-Tedious pre-treatment process -Small linear concentration range -Polishing is needed -Electrode Poisoning with time	[14]	0.5 M NaNO$_3$–HNO$_3$, pH 1.0	Tablet	0.93	2.0 – 41	ATN	**BDE**
-Multistep fabrication process -Difficult to apply in-field -Small linear concentration range -Expensive electrode materials -Polishing is needed -Electrode Poisoning with time	[18]	B.R. buffer pH 9.5	––	0.39	1- 100	ATN	**poly(glutamic) acid/cysteine/Au NPs/GCE**
-Tedious fabrication process -Difficult to apply in-field -Expensive electrode -Polishing is needed -Electrode Poisoning with time	[16]	0.1 M PBS (pH 7.0) + 10 mM CTAB	Tablet	0.004	0.01 – 4	NIF	2 PdAg/graphene nanoribbons/GCE
-Tedious fabrication process -Difficult to apply in-field -low stability -Polishing is needed	[21]	B.R. buffer pH 1.5	Tablet Urine	0.015	0.048 –20	NIF	**β-cyclodextrin/MWCNT**
-Tedious fabrication process -Difficult to apply in-field -Expensive electrode materials -Polishing is needed -Electrode Poisoning with time	[19]		Tablet Urine	0.72	0.8–60.0	NIF	3 Ag NPs/GCE
-Large scale electrode production -Simple fabrication process -Wide linear concentration range -Reproducible and stable electrode in real samples - disposable electrode - Economic electrode materials	This work	B.R. buffer pH 9	Tablet Urine	1.76	6.67 – 909	ATN	**MgO-SPEs**
				0.032	0.2–104.4	NIF	

NPs: nanoparticles; MWCNT: multiwalled carbon nanotube; BDE: boron diamond doped electrode; CP: carbon past.

7 and pH 9 respectively. It can be seen that with increasing the concentrations of NIF and ATN, the oxidation peak heights were linearly increased. The linear calibration plot of NIF (Fig. 5b) was obtained from the analysis voltammograms over concentration range of 0.20–104.41 μM; $I_P/\mu A = 0.06C_{NIF}/\mu M + 0.21\,\mu A$; $R^2 = 0.99$; $N = 3$. The analysis of the voltammetric peak current of ATN reveals two linear responses (Fig. 5d); $I_P\,(\mu A) = 0.013C_{ATN}/\mu M + 0.18\,\mu A$; $R^2 = 0.993$; $N = 3$ and $I_P\,(\mu A) = 0.006C_{ATN}/\mu M + 3.9\,\mu A$; $R^2 = 0.99$; $N = 3$. Based on the standard deviation of the intercept and the average slope of the linear calibration range, the limits of detection were estimated to be 0.032 μM and 1.76 μM for NIF and ATN respectively. To the best of our knowledge, NIF and ATN are conjugated in several pharmaceutical formulations but there is no published work for simultaneous voltammetric determination of NIF and ATN in tablets or biological fluids (Table 2).

3.5. Simultaneous determination of NIF and ATN using MgO-SPEs

Next, attention was turned to determination of NIF in presence of ATN. Fig. 6a shows the consecutive additions of NIF in the range of 1.7 – 63 μM in presence of 385 μM ATN in B.R. buffer pH 9. Interestingly, the oxidation peak current of ATN was almost constant with an RSD = 2.33%. The linear relationship of peak current and NIF additions can be described as follows; $I_P\,(\mu A) = 0.07C_{NIF}/\mu M + 0.047\,\mu A$; $R^2 = 0.99$; $N = 3$. Additions of ATN concentrations in the range of 33–1170 μM in presence of 20 μM NIF in B.R. buffer pH 9 is depicted in Fig. 6B. The oxidation

peak current of NIF was remained constant with RSD = 1.09%. The analysis of the peak height with concentration of ATN can be presented as $I_P\,(\mu A) = 0.0129C_{ATN}/\mu M + 0.19\,\mu A$; $R^2 = 0.996$; $N = 3$ and $I_P\,(\mu A) = 0.0048C_{ATN}/\mu M + 4.6\,\mu A$; $R^2 = 0.99$; $N = 3$. These results revealed that, there is no significant interference from each analyte in the simultaneous determination of its pairs. It is very important to note that, the electrochemical oxidation processes of ATN and NIF antihypertensive drugs are independent onto MgO- SPE. Further, NIF and ATN were also determined by simultaneously changing their concentrations in BR buffer solution of pH 9. Fig. 7 shows DPV for continuous additions of both NIF and ATN unitizing MgO NPLs as nanozyme materials. The analysis of NIF voltammetric peak current reveals a linear response (Fig. 7b) in range of 1.3–101 μM with corresponding calibration equation; $I_P\,(\mu A) = 0.063C_{NIF}/\mu M + 0.13\,\mu A$; $R^2 = 0.994$; $N = 3$. On other hand, the analysis of ATN voltammetric peak current represents also a linear response (Fig. 7c) over the range of 6.67–500 μM; $I_P\,(\mu A) = 0.0125C_{ATN}/\mu M + 0.067\,\mu A$; $R^2 = 0.99$; $N = 3$. As shown, MgO-SPEs show promising electrode material for simultaneous determination of NIF and ATN because they offered sensitivity, stability, reproducibility, and economical compared with previous literatures (Table 2).

3.6. Accuracy, repeatability and robustness of MgO-SPEs

The DPV method was validated according to ICH [45] guidelines 2005 and complied with USP [46] on the validation of analytical methods. Accuracy is measured by adding known amounts of the
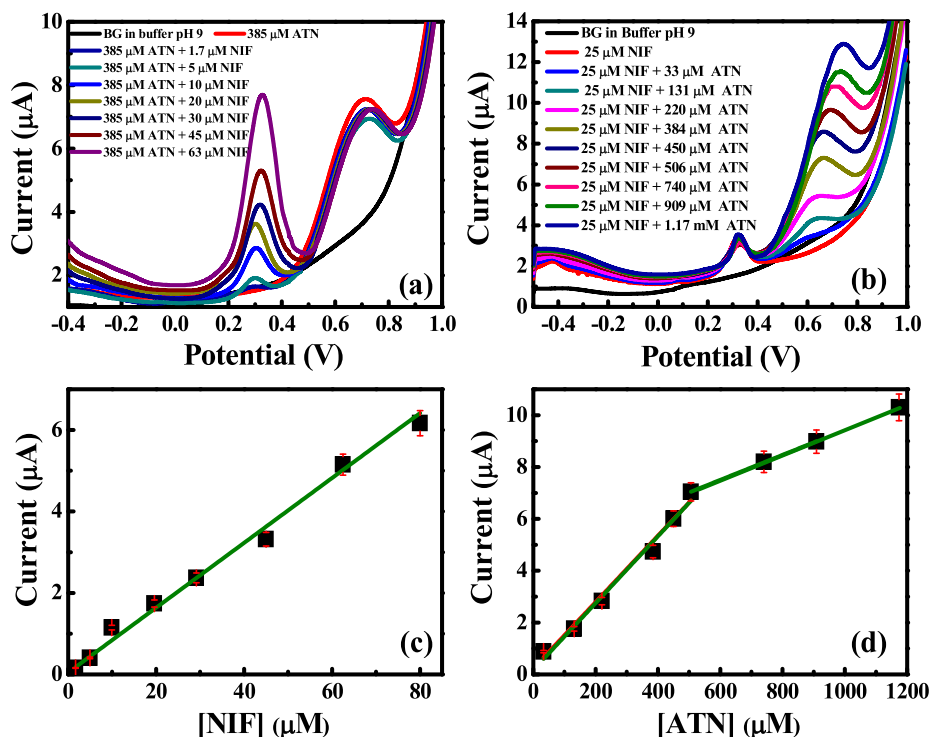
Fig. 6. (a) DPV curves for additions of NIF in the presence of 385 μM ATN, (b) additions of ATN in presence of 25 μM NIF, Linear correlation of peak currents and concentrations of (c) NIF and (d) ATN in BR buffer solution of pH 9.0 using MgO − SPEs.

Table 3
Accuracy of the proposed voltammetric method.

% Recovery ± SD[a]	Total Amount Found [μM]	Amount Added [μM]	Amount Taken [μM]	Drug
100. 59 ± 1.76	15.09	4.62	9.24	**NIF**
98.68 ± 1.76	19.74	9.24	9.24	
98.83 ± 2.62	24.71	13.68	9.24	
98.10 ± 2.55	3.75	15	30	**ATN**
98.37 ± 1. 92	19.67	30	30	
101.05 ± 3.35	25.03	45	30	

[a] Average of 6 determinations.

Table 4
Inter- and Intra-day precision of the proposed method.

Inter-day RSD% [b]	Intraday RSD% [a]	Conc. [μM]	Drug
2.76	2.06	0.33	**NIF**
1.98	1.51	15	
2.72	2.96	39.51	
2.34	1.56	6.62	**ATN**
0.67	1.08	100	
2.89	2.31	866.1	

[a] Average of 6 determinations.
[b] Average of 18 determinations over 3 days.

Table 5
Robustness of the proposed voltammetric method.

Recovery (%) ± SD[a]		Experimental parameter
ATN	NIF	
99.93 ± 1.96	99.67 ± 1.78	Optimal parameters
98.45 ± 1.56	100.92 ± 0.98	Starting Potential
100.98 ± 2.45	98.78 ± 2.05	−0.52
		−0.48
97.96± 2.45	98.67 ± 1.91	Modulation Amplitude
101.53 ± 1.58	97.95 ± 2.21	0.0705
		0.0695
98.67 ± 1.97	98.31 ± 1.89	Modulation Time
99.45 ± 2.25	99.56 ± 1.65	0.0495
		0.0505
103.97 ± 2.79	98.78 ± 0.83	Step Potential
98.15± 1.69	101.41 ± 2.31	0.0495
		0.0505
98.29 ± 1.88	101.57 ± 1.46	Interval Time
97.64 ± 2.26	98.19 ± 2.41	0.495
		0.505

[a] Average of 3 determinations.

standard NIF and ATN (at three concentration levels 50%, 100% and 150%) to pre-analysed tablet samples according to the ICH guidelines. After dilution of drugs to the recommended concentrations of the investigated drugs, six separated solutions were analysed by the proposed method. The results were obtained using standard addition protocol and they were satisfactory as indicated in Table 3. The recovery experiments were carried out by adding 9.24 μM and 30 μM of NIF and ATN solutions prepared from commercial products to 15.0 mL of B. R buffer pH 9 followed by standard additions of each stock solutions. The recoveries of known amounts of NIF and ATN contained in pharmaceutical formulations are given in Table 3. The estimated recoveries were ranged from 97.10% to 100.90%, indicating an acceptable accuracy of the DPV method.

Intra-day repeatability was estimated by measurement of six replicates of three concentration levels covering the low, medium, and high concentration ranges of each calibration plot. Inter-day
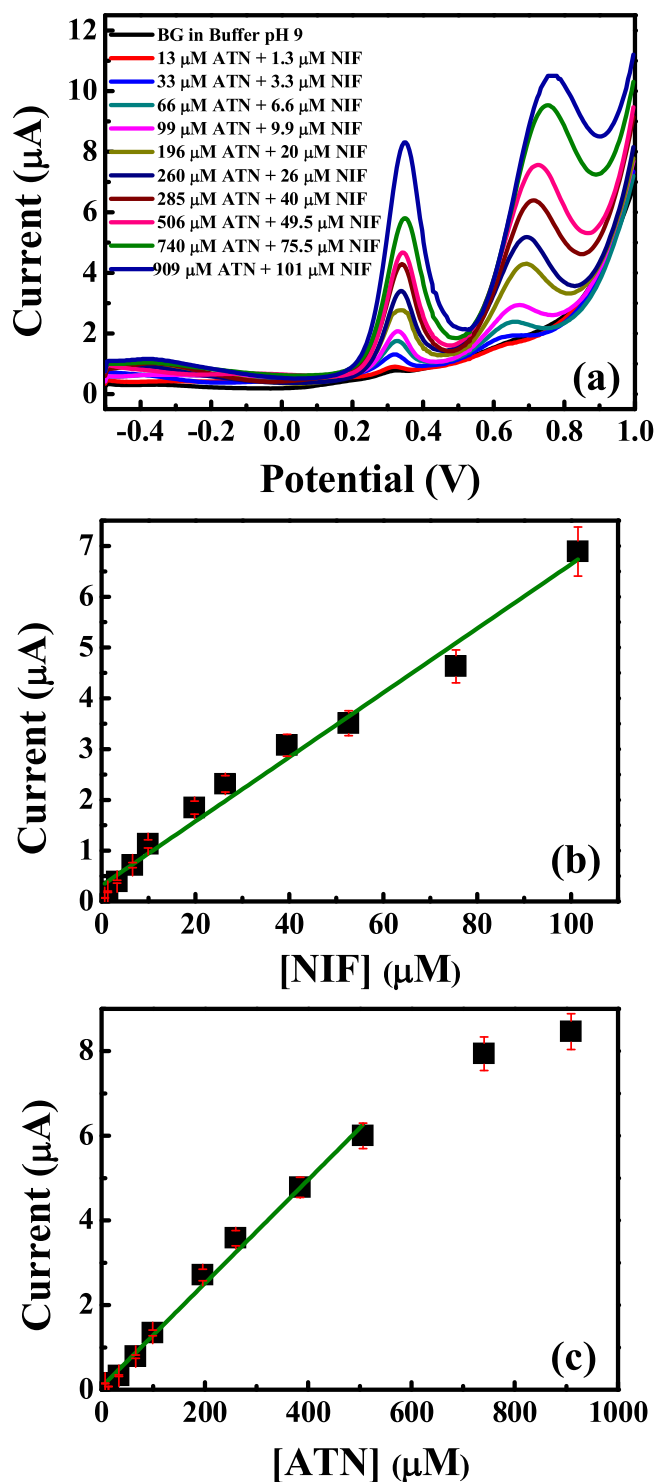
Fig. 7. (a) DPV curves for the simultaneous determination of NIF and ATN in B.R. buffer pH 9, (b) linear correlation of oxidation peak current of NIF against its concentrations, (c) linear correlation of oxidation peak current of ATN against its concentration of ATN. [DPV parameters: Step potential = 0.005 mV, modulation amplitude = 0.07 V modulation time 0.05 s, interval time = 0.1s, scan rate = 0.05 mVs^{-1}].

Table 6
Application of the proposed voltammetric method for determination of the studied drugs in commercial tablets.

F-value	t-value	Recovery%± SD[a] HPLC [24]	Recovery%± SD[a] Proposed method	Dosage form (tablet)	
1.32	1.75	97.22 ± 1.25	98.40 ± 1.08	NIF	
1.23	0.38	98.13 ± 1.94	98.53 ± 1.75	ATN	NIF+ ATN (Tenolat SR)

Theoretical values at 95% confidence limit; t = 2.30 F = 5.05.

[a] Average of six determinations.

Table 7

Application of the proposed voltammetric method for determination of the studied drugs in Urine sample.

Recovery% ± SD[a]	Found conc. [μM]	Added conc. [μM]	Drug
92.56 ± 3.32	0.185	0.2	**NIF**
93.46 ± 1.97	4.67	5	
91.69 ± 3.56	9.17	10	
94.21 ± 3.74	6.283	6.67	**ATN**
95.41 ± 1.61	14.31	15	
93.91 ± 2.93	28.17	30	

[a] Average of six determinations.

variation was evaluated due to measure drug repeatedly with the same concentration over a period of three days intra-day and inter-day precision were expressed as percent relative standard deviation (% RSD) the results were given in Table 4. For all concentration levels, the RSD didn't exceed 2.96% indicating good precision. The robustness of the analytical procedure is a measure of its capacity to remain unaffected by small but deliberate variation in the method parameters and provide indication of its reliability during normal usage. A small variation in the DPV method parameters did not affect the voltammetric response significantly as shown in Table 5. This result indicates that, MgO-SPE showed high robustness for simultaneous determination of NIF and ATN in real samples.

3.7. Analysis of real samples

The applicability of MgO-SPEs for simultaneous voltammetric determination of NIF and ATN in real samples has been explored in a dosage form Tenolat SR tablet; containing 20 mg NIF and 50 mg ATN and urine samples. Six replicate measurements have been performed for each concentration. The results have been depicted in Tables 6 and 7. Interestingly, the voltammetric methodology for simultaneous determination of NIF and ATN by utilizing MgO-SPEs show a satisfactory results compared with reported HPLC method. No significant difference was found by applying t- and F- tests at 95% confidence level, indicating high accuracy, precision and suitability of MgO-SPEs for sensitive determination of the NIF and ATN antihypertensive drugs simultaneously in pharmaceutical formulations.

The recovery experiment for NIF and ATN in collected urine samples have been performed by addition of 0.5 mL of urine sample to 14.5 mL B.R. buffer pH 9. The spiked NIF and ATN concentrations have been measured via standard addition protocol as shown in Table 7. These results revealed that MgO-SPEs are a promising electrode for simultaneous determination of NIF and ATN in urine matrix with excellent recoveries percentage.

4. Conclusions

We report, for the first time, simultaneous voltammetric determination of NIF and ATN anti-hypertensive drugs by utilizing MgO NPLs modified SPEs. The studied drugs are formulated together in single pharmaceutical dosage forms. The results have shown that MgO-SPEs are a promising disposable electrode for the fabrication of a highly sensitive electrochemical sensor for simultaneous detection of NIF and ATN. The merits of the SPEs as the basis of the sensor can be also taken into consideration such as: low cost, easy construction and storage, potential for miniaturization, facility of automation and construction of simple and portable equipment. Furthermore, adequate recovery results were obtained for the simultaneous determination of NIF and ATN in spiked human urine sample, indicating that the proposed voltammetric method can be applied to routine analysis.

Appendix A. Supplementary data

Supplementary data associated with this article can be found, in the online version, at http://dx.doi.org/10.1016/j.snb.2017.06.105.

References

[1] R.A. Harvey, P.C. Champe, M.J. Mycek, S.B. Gertner, M.M. Perper, Lipincott's illustrated reviews, Pharmacology (1992) 181–184.
[2] W.C. Cushman, C.E. Ford, P.T. Einhorn, J.T. Wright Jr., R.A. Preston, B.R. Davis, J.N. Basile, P.K. Whelton, R.J. Weiss, A. Bastien, D.L. Courtney, B.P. Hamilton, K. Kirchner, G.T. Louis, T.M. Retta, D.G. Vidt, J. Clin. Hypertens 10 (2008) 751–760.
[3] M. Doménech, A. Coca, J. Patient Prefer Adherence 4 (2014) 105–113.
[4] A.H. Gradman, J.N. Basile, B.L. Carter, G.L. Bakris, J. Am. Soc. Hypertens 4 (2010) 42–50.
[5] S.C. Sweetman, Martindale; The Complete Drug Reference, 33rd edition, Pharmaceutical Press, London, 2002, pp. 921–922.
[6] N.P. Chau, X. Chanudet, G. Nguyen, Curr. Ther. Res. 52 (1992) 906–915.
[7] T. Godfraind, R. Miller, M. Wibo, Pharmacol. Rev. 38 (1986) 321–416.
[8] W. H.Winkler, B. Ried, J. Lemmer, Chromatogr. Biomed. Appl. 228 (1982) 223–234.
[9] K.M. Al Azzam, B. Saad, H.Y. Aboul-Enein, Biomed. Chromatogr. 24 (2010) 977–981.
[10] E.A. Abdel Hameed, R.A. Abdel Salam, G.M. Hadad, Spectrochim. Acta A 141 (2015) 278–286.
[11] X. Tan, J. Yang, Q. Li, Q. Yang, Y. Shen, Spectrochim. Acta 161 (2016) 19–26.
[12] P.C. Damiani, Talanta 85 (2011) 1526–1534.
[13] A. Khataee, R. Lotfi, A. Hasanzadeh, M. Iranifam, S.W. Joo, Spectrochim. Acta 157 (2016) 88–95.
[14] E.R. Sartori, R.A. Medeiros, R.C. Rocha-Filho, O. Fatibello-Filho, Talanta 81 (2010) 1418–1424.
[15] R. Afonso, A.P.P. Eisele, J.A. Serafim, A.C. Lucilha, E.H. Duarte, C.R.T. Tarley, E.R. Sartori, L.H. Dall'Antonia, J. Electroanal. Chem. 765 (2016) 30–36.
[16] L. Shang, F. Zhao, B. Zeng, Electrochim. Acta 168 (2015) 330–336.
[17] M. Arvand, M. Vaziri, M. Vejdani, Mater. Sci. Eng. C 30 (2010) 709–714.
[18] S. Pruneanu, F. Pogacean, C. Grosan, E.M. Pica, L.C. Bolundut, A.S. Biris, Chem. Phys. Lett. 504 (2011) 56–61.
[19] N. Shadjou, M. Hasanzadeh, L. Saghatforoush, R. Mehdizadeh, A. Jouyban, Electrochim. Acta 58 (2011) 336–347.
[20] M. Baghayeri, M. Namadchian, H. Karimi-Maleh, H. Beitollahi, J. Electroanal. Chem. 697 (2013) 53–59.
[21] R.R. Gaichore, A.K. Srivastava, Sens. Actuators B 188 (2013) 1328–1337.
[22] L. Xu, Q. Guo, H. Yu, J. Huang, T. You, Talanta 97 (2012) 462–467.
[23] I. Abdallah, A. Ibrahim, N. Ibrahim, M. Rizk, S. Tawakkol, Pharm. Anal. Acta 6 (2015) 1–9.
[24] B.L. Bing, H. De-fu, L. Fei, J. Chinese, Pharm. Anal. 24 (2004) 485–486.
[25] R.R. Kallem, J.K. Inamadugu, M. Ramesh, J. Seshagirirao, Biomed. Chromatogr. 27 (2013) 349–355.
[26] M. Pumera, S. Sanchez, I. Ichinose, J. Tang, Sens. Actuators B 123 (2007) 1195–1205.
[27] C.M. Welch, R.G. Compton, Anal Bioanal. Chem. 384 (2006) 601–619.
[28] X. Luo, A. Morrin, A.J. Killard, M.R. Smyth, Electroanalysis 18 (2006) 319–326.
[29] Z. Dohnálek, G.A. Kimmel, D.E. McCready, J.S. Young, A. Dohnálková, R.S. Smith, B.D. kay, J. Phys. Chem. B 106 (2002) 3526–3529.
[30] K. Mageshwari, S.S. Mali, R. Sathyamoorthy, P.S. Patil, Powder Technol. 249 (2013) 456–462.
[31] D.S. Seferos, D.A. Giljohann, H.D. Hill, A.E. Prigodich, C.A. Mirkin, J. Am. Chem. Soc. 129 (2007) 15477–15479.
[32] (a) W.J. Parak, T. Pellegrino, C. Plank, Nanotechnology 16 (2005) R9;
(b) Y. Zhang, H. He, B. Pan, J. Phys Chem. C 116 (2012) 23130–23135.
[33] D.J. Lyell, K. Pullen, L. Campbell, S. Ching, M.L. Druzin, U. Chitkara, D. Burrs, A.B. Caughey, Y.Y. El-Sayed, Obstet. Gynecol. 110 (2007) 61–67.
[34] M. Li, Y.-T. Li, D.-W. Li, Y.-T. Long, Anal. Chim. Acta 734 (2012) 31–44.
[35] M. Khairy, A.A. Khorshed, F.A. Rashwan, G.A. Salah, H.M. Abdel-Wadood, C.E. Banks, Sens. Actuators B 239 (2017) 768–775.
[36] B.G. Mahmoud, M. Khairy, F.A. Rashwan, C.W. Foster, C.E. Banks, RSC Adv. 6 (2016) 14474–14482.
[37] L.M. Ochiai, D. Agustini, L.C. Figueiredo-Filho, C.E. Banks, L.H. Marcolino-Junior, M.F. Bergamini, Sens. Actuators B 241 (2017) 978–984.
[38] S. Rana, S.K. Mittal, N. Singh, J. Singh, C.E. Banks, Sens. Actuators B 239 (2017) 17–27.
[39] R.S. Nicholson, Anal. Chem. 37 (1965) 1351–1355.
[40] S.J. Rowley-Neale, D.A.C. Brownson, C.E. Banks, Nanoscale 8 (2016) 15241–15251.
[41] B.G. Mahmoud, M. Khairy, F.A. Rashwan, C.E. Banks, Anal. Chem. 89 (2017) 2170–2178.

[42] M. Khairy, S.A. El-Safty, RSC Adv. 3 (2013) 23801–23809.
[43] B. Weintraub, Z. Zhou, Y. Li, Y. Deng, Nanoscale 2 (2010) 1573–1587.
[44] M. Behpour, E. Honarmand, S.M. Ghoreishi, B. Korean Chem. Soc. 31 (2010) 845–849.
[45] I.C.H. Harmonised Tripartite Guideline, Validation of Analytical Procedures: Text and Methodology Q2 (R1), 2005, Geneva.
[46] United States Pharmacopeia USP31- NF26, U S, Pharmacopiea Convention Inc, Twinbrook Parkway, Rockville, MD, 2008, 813–814, 1669–1671, 2256–2258.

Biographies

Mohamed Khairy received his PhD in Chemistry (Nanodevice) from Waseda University, Tokyo, Japan in 2013. He was a postdoc researcher at national institute for material science in 2014. Currently, he is working as lecturer in Chemistry Department Faculty of Science, Sohag University, Sohag, Egypt. His current research interests are control synthesis of porous metal oxide nanostructures for developing electrochemical sensors.

Craig E. Banks is a Professor of Chemistry at Manchester Metropolitan University and has published over 360 papers with a h-index over 55 (Web of Science, June2017). He has written 5 books, contributed 18 book chapters and is an inventor of 17 patents. His current research is directed toward the pursuit of studying the fundamental understanding and applications of nano-electrochemical systems such as graphene, carbon nanotube and nanoparticle derived sensors and developing novel electrochemical sensors *via* screen printing and related techniques.